THE INTERPRETATION OF PAPER PROPERTIES IN TERMS OF STRUCTURE

H. CORTE AND O. J. KALLMES

WIGGINS TEAPE RESEARCH AND DEVELOPMENT LTD., BEACONSFIELD
AND ST. REGIS PAPER CO., WEST NYACK, N.Y., U.S.A.

Synopsis

The physical properties of paper have been interpreted on the basis of the theory of the statistical geometry of fibrous networks. One example of each of the three main groups of properties is discussed: the maximum pore size and the optically bonded area on the basis of the theory of multi-planar structures and of the number of bond failures in the fracture of random two-dimensional networks. The experimental results support the statistical geometric approach to structure and physical properties.

L'interprétation des propriétés du papier en termes de sa structure

On présente une interprétation des propriétés physiques du papier en se basant sur la théorie de la géometrie statistique des réseaux fibreux.

On étudie un exemple de chacun des trois principaux groupes de propriétés du papier—la dimension du plus grand pore et l'étendu de la surface en contact optique en se basant sur la théorie des structures multi-planaires et le nombre de liaisons détruites lors de la rupture des réseaux bi-dimensionnels organisés au hazard.

Les résultats expérimentaux justifient l'interprétation des propriétés physiques et structurales au moyen de la géometrie statistique.

24—F.S.P.: i

Die Deutung der Eigenschaften von Papier auf Grund seiner Struktur

Die physikalischen Papiereigenschaften werden auf Grund der statistischen Geometrie von Fasernetzwerken gedeutet. Von den drei Hauptgruppen physikalischer Eigenschaften—Porositätseigenschaften, optischen und mechanischen Eigenschaften, wird je ein Beispiel diskutiert und zwar die maximale Porengrösse und die optische Kontaktfläche mit Hilfe der Theorie multiplanarer Strukturen sowie die Zahl der zerstörten Faserbindungen beim Zerreissen einer zufällig angeordneten zweidimensionalen Struktur. Die experimentellen Ergebnisse rechtfertigen den Versuch, Struktur und physikalische Eigenschaften statistisch-geometrisch zu behandeln.

Introduction

PAPER first came into general usage when man found in it a thin, planar material of considerable mechanical strength with a closed smooth surface on which he could write and, centuries later, print. In the Damascus bazaars of the eleventh century, he first took advantage of its folding endurance to use it also as a protective wrapping material. As civilisation has become more and more complex, the types of paper used have increased accordingly. In many present applications, paper properties other than those of structure are of prime importance—for example, the hygroscopic properties of cellulose have made it impossible to form a watervapourproof structure, hence the marriage of paper and plastics. Its lack of certain chemicals determines its quality for use as a photographic base paper. Yet it is difficult to find a single application in which structural properties are not of major importance in themselves or are a cause of certain physical characteristics.

All papermaking problems may be said to begin with the job of selecting those fibres that will assure the desired macroscopic paper properties. This is because many characteristics of the individual fibres are reflected in the gross paper properties. We believe that the arrangement of the fibres in the sheet, the paper structure, is the key link between the fibre and sheet properties. To this end, we have been engaged for some time in studies aimed at describing paper structure.[1, 2] In this article, we will show how the concepts of sheet structure may be employed to relate fibre properties to an example of each of the main types of sheet property—porous, optical and mechanical.

Porous properties

Maximum pore size

WE seek to describe the porous properties of paper only with geometric laws and physical laws of the behaviour of fluids. As in our treatment of the fibre arrangement in paper, our work with porosity began with ultra-thin, 2-D sheets, whose pores are irregular polygons lying in a single plane; an approximate expression for their size distribution was worked out without much difficulty,[1] though there is an insurmountable conceptual problem right in the first step of describing the pores in a three-dimensional network—the definition of a pore. If three-dimensional pores are to be mathematised at all, they must be defined in models better suited to quantitative descriptions than real paper. The multi-planar (MP) model appeared to be the most suitable for reasons that will become evident later; its use was justified by a four-factor analysis of variance that showed MP sheets not significantly different from normally formed handsheets in specific volume, elastic modulus and breaking load and stretch. Their stress/strain curves are in fact almost identical.

In the schematic cross-section of an MP sheet in Fig. 1, the fibres, lying in specific layers, appear as rectangles of exaggerated, uniform height and irregular lengths, spaced with irregular gaps. The gaps are cross-sections of irregular polygons and N_L of them in vertical sequence form a tortuous pore of variable cross-sectional area (N_L is the number of 2-D layers in an MP sheet). Laminar flow of a fluid through a pore such as a in Fig. 1 may be primarily controlled by its average cross-sectional area, its capillary flow by the mean reciprocal diameter.

The above approach to porosity phenomena was initially applied to the so-called 'first bubble experiment', because it is static and involves geometric laws only; complications due to fluid flow are not encountered. This is the experiment in which the air pressure below a sheet is increased by increments against a constant head of liquid above it until the first air bubble is forced through. The smallest of the N_L polygons within each pore is the bottleneck where air pressure must outstrip the surface tension of the liquid; the largest of the bottleneck polygons is the one through which the first bubble will pass. The pressure at which this first bubble appears depends on the cross-sectional area of the largest of the bottleneck polygons.

One reason that the MP approach was found useful here is that the cross-sectional area of the largest bottleneck polygon can be calculated from this model. Neglecting for the moment the cases of blocking and splitting (b and s in Fig. 1) results in a structure with as many bottleneck polygons as holes in one layer.

The mathematics used to determine the size of the largest bottleneck polygon is based on the theory of extreme values[3] and uses the following notation—

x = area of polygons $(a_h^{(1)})$

n = number of polygons in one 2-D layer $(N_h^{(1)})$

m = number of layers in $(N_L^{(2)})$

a = constant.

The polygon size distribution in a single 2-D layer is—

$$f(x) = \frac{ae^{-a\sqrt{x}}}{2\sqrt{x}} \, dx \quad \cdot \quad \cdot \quad \cdot \quad \cdot \quad \cdot \quad \cdot \quad (1)$$

which when integrated gives the cumulative distribution—

$$F(x) = 1 - e^{-a\sqrt{x}} \quad \cdot \quad \cdot \quad \cdot \quad \cdot \quad \cdot \quad (2)$$
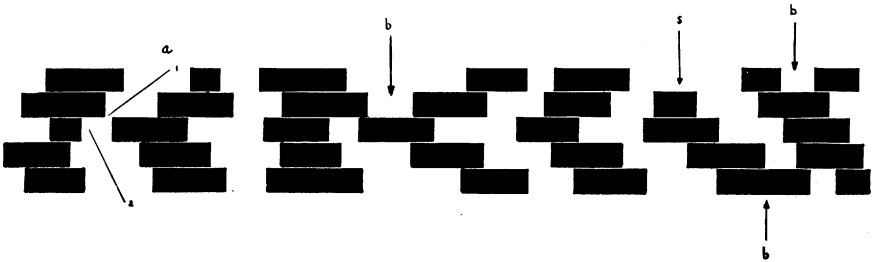

Fig. 1—Schematic cross-section through a multi-planar sheet

The m polygons of each pore constitute a sample of size m from a population having the distribution given by equation (1). From extreme value theory, the cumulative distribution of the smallest areas, denoted by x_1, in samples of size m, is—

$$\Phi_{1,m}(x_1) = 1 - [1 - F(x_1)]^m \quad \cdot \quad \cdot \quad \cdot \quad \cdot \quad (3)$$

Combining (2) and (3),

$$\Phi_{1,m}(x_1) = 1 - e^{-ma\sqrt{x_1}} \quad \cdot \quad \cdot \quad \cdot \quad \cdot \quad (4)$$

The bottleneck polygons of the sheet are a sample of size n from a population with the distribution given by equation (4). Its *expected largest value*, denoted $x_{1,n}$, is defined by—

$$\Phi_{1,m}(x_{1,n}) = 1 - \frac{1}{n} \quad \cdot \quad \cdot \quad \cdot \quad \cdot \quad \cdot \quad (5)$$

Applying this definition to equation (*4*), gives—

$$e^{-ma\sqrt{x_{1,n}}} = \frac{1}{n} \qquad \ldots \ldots \ldots (6)$$

The term $x_{1,n}$ is identical to the experimentally determined largest pore area x_m. From equation (*6*)—

$$x_m = \frac{1}{m^2 a^2} (\log_e n)^2 \qquad \ldots \ldots \ldots (7)$$

Rewriting equation (*7*) in terms of the maximum pore radius, r_m—

$$r_m = \frac{1}{ma\sqrt{\pi}} \log_e n \qquad \ldots \ldots \ldots (8)$$

The term r_m can be calculated directly from equation (*8*), because m, a and n are known.[1] In terms of our usual notation, the constant a is—

$$a = \frac{N_f \bar{\lambda}}{A\bar{\tau}} \sqrt{\frac{2}{\pi}}, \qquad \ldots \ldots \ldots (9)$$

(*see* equations (*12*), (*26*), (*28a*)[1]).

The values $\bar{\lambda}$ and $\bar{\tau}$ are, respectively, the mean fibre length and curl; A the sample area; N_f the number of fibres in a 2-D layer. Introducing the relationship between the sheet basis weight W and specific fibre weight w (the mass per unit length of fibre)—

$$W = \frac{mN_f \lambda w}{A}$$

into equation (*8*) gives—

$$ma = \frac{W}{\bar{\tau} w} \sqrt{\frac{2}{\pi}} \qquad \ldots \ldots \ldots (10)$$

Equations (*8*) and (*10*) combine to give—

$$r_m = \frac{\bar{\tau} w}{\sqrt{2} W} \log_e N_h \qquad \ldots \ldots \ldots (11)$$

or

$$r_m W = \frac{\bar{\tau} w}{\sqrt{2}} \log_e N_h \equiv K \qquad \ldots \ldots \ldots (12)$$

According to equation (*12*), the maximum pore size is inversely proportional to the basis weight—that is, $r_m W$ is equal to a constant K. For a

given basis weight, the maximum pore radius is almost proportional to the specific fibre weight, meaning that the heavier the fibres, the fewer the number in a given weight and the fewer and larger the pores.

From Corte and Kallmes,[1] $N_h = (N_c - N_f) \exp(-N_f \bar{\lambda} \bar{\omega}/A)$ and $N_c = (N_f \bar{\lambda})^2 / \pi A \bar{\tau}^2$, where N_c is the number of crossings in one 2-D layer of area

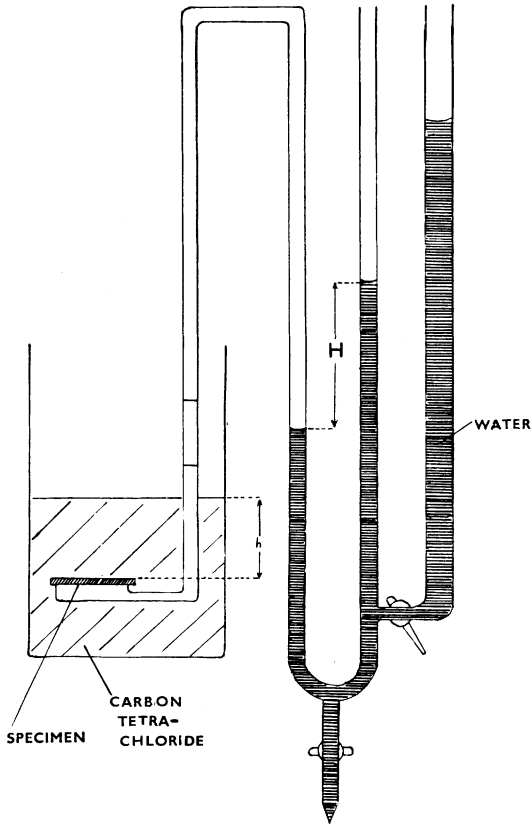*Fig. 2*—Apparatus to determine the maximum pore radius

A and $\bar{\omega}$ is the mean fibre width. Introducing $G = N_f \bar{\lambda} w/A$, the basis weight of a 2-D layer, produces—

$$K = \frac{2 \cdot 3}{\sqrt{2}} \bar{\tau} w \left[\log \frac{GA}{w} + \log \left(\frac{G}{\pi \bar{\tau}^2 w} - \frac{1}{\bar{\lambda}} \right) - 0 \cdot 43 \frac{G \bar{\omega}}{w} \right] \quad . \quad . \quad (13)$$

Equation (13) is an expression for a physical property, the maximum pore radius as measured in the first bubble experiment, in terms of geometric laws and fibre dimensions only.

The experimental determination (*see* Fig. 2) of r_m is based on the well-known Kelvin equation—

$$r_m = \frac{2\sigma}{g(H - \rho h)} \qquad \ldots \ldots \quad (14)$$

The terms σ and ρ are, respectively, the surface tension (25·7 dyn/cm) and density (1·6) of carbon tetrachloride, the liquid we used in the experiment; H is the pressure drop in the manometer in cm of water; h is the head of carbon tetrachloride above the sample (1·0–1·5 cm); g is the gravitational constant. The experiment was performed on the central 11·1 cm² of 12·9 cm² samples. Water was added in small amounts from the reservoir to the manometer to build up the pressure under the sample slowly until the first bubbles appeared through one point of the sheet. The term r_m is the radius of a circle of about the same area as the largest pore. For further discussion on non-circular pores, see Scheidegger.[4]

Tests of equation (*12*) were carried out on four bleached pulps (*see* Table 1 for their properties), before and after one or several beating intervals in a Clough beater. Four and, in one case, five different weights of sheet, each replicated six times, were prepared from every pulp by the standard procedure, slightly modified in that the sheets were pressed at 100 lb/in² for only one 5 min period.

Fibres of normally formed sheets do not occur in specific layers as in MP sheets and, since the former was the only kind of sheet tested, the basis weight per 'layer', G, had to be decided arbitrarily. The sheets were dense in structure, hence the choice of 1 g/m². (K is not very sensitive to variations in G, because it is a function of the logarithm of G.)

Among the K values of Table 2, the calculated values are generally larger than the experimental values, but the difference is small in view of the non-ideality of the beaten pulps. The experimental K readings of the softwood pulps are reasonably constant at each degree of beating and decrease with beating time as the sheets become denser.

At most beating intervals, the experimental K figures of the softwoods showed only a slight tendency to decrease with increasing basis weight; however, this effect becomes pronounced in hardwoods. It appeared to us that the blocking effect (*see* pore *b* in Fig. 1) may have caused this discrepancy and, if so, equation (*12*) becomes—

$$r_m W = K + EW \qquad \ldots \ldots \quad (15)$$

TABLE 1

Softwood sulphate I					Softwood sulphate II					Softwood sulphite					Hardwood semi-chemical				
°S.R.	λ	$\bar{\tau}$	$\bar{\omega}$	w	°S.R.	λ	$\bar{\tau}$	$\bar{\omega}$	w	°S.R.	λ	$\bar{\tau}$	$\bar{\omega}$	w	°S.R.	λ	$\bar{\tau}$	$\bar{\omega}$	w
14	0·283	1·21	3·90	2·36	16	0·157	1·013	3·45	2·40	15	0·156	1·100	3·65	1·80	23	0·070	1·139	1·41	1·10
					25	0·142	1·011	3·15	2·30	17	0·152	1·099	3·52	1·76	26	0·065	1·107	1·46	1·16
					34	0·132	1·009	3·17	2·25	23	0·142	1·088	3·33	1·68	38	0·063	1·027	1·54	1·27
					44	0·124	1·008	3·19	2·23	30	0·131	1·077	3·15	1·59	45	0·057	1·035	1·56	1·14
										42	0·108	1·066	3·00	1·45					

$\bar{\lambda}$ = mean fibre length, cm
$\bar{\tau}$ = mean curl factor
$\bar{\omega}$ = mean fibre width, cm$\times 10^3$
w = specific fibre weight, g/cm$\times 10^6$

TABLE 2

*Softwood sulphate I

°S.R.	W	$r_m \times 10^4$	K exp.	K calc.
14 un-beaten	13·0	147·6	0·191	0·156
	29·0	54·4	0·158	
	44·1	33·9	0·150	
	59·4	25·2	0·150	
	96·9	19·7	0·191	

* Replicated 50 times

Softwood sulphate II

°S.R.	W	$r_m \times 10^4$	K exp.	K calc.
16 un-beaten	20·6	62·5	0·129	0·136
	34·0	34·6	0·118	
	56·0	22·8	0·128	
	68·4	18·9	0·129	
25	22·3	54·5	0·122	0·130
	44·1	23·6	0·104	
	80·4	14·3	0·115	
	92·1	12·6	0·116	
34	17·6	60·6	0·107	0·127
	36·7	26·3	0·097	
	54·2	18·2	0·098	
	73·7	13·4	0·098	
44	15·1	74·8	0·113	0·124
	31·4	27·5	0·086	
	56·6	16·4	0·093	

Softwood sulphite

°S.R.	W	$r_m \times 10^4$	K exp.	K calc.
15 un-beaten	17·4	60·1	0·104	0·116
	30·0	42·2	0·124	
	52·0	20·6	0·107	
	67·0	15·4	0·104	
17	19·2	52·2	0·100	0·114
	43·8	23·6	0·103	
	58·4	14·3	0·084	
	85·8	10·2	0·087	
23	18·2	56·0	0·102	0·110
	38·1	24·2	0·092	
	57·5	16·3	0·093	
	87·3	12·0	0·105	
30	16·6	59·6	0·099	0·104
	34·5	28·6	0·099	
	47·5	20·3	0·097	
	69·0	10·6	0·073	
42	14·2	53·7	0·076	0·095
	37·7	16·8	0·063	
	53·3	13·0	0·069	
	68·2	10·5	0·072	

Hardwood semi-chemical

°S.R.	W	$r_m \times 10^4$	K exp.	K calc.
23 un-beaten	16·0	53·7	0·085	0·078
	20·3	34·5	0·070	
	26·2	26·2	0·069	
	27·6	21·6	0·060	
26	18·7	65·8	0·122	0·079
	22·0	35·7	0·079	
	27·6	25·0	0·069	
	28·7	23·5	0·067	
38	14·7	72·5	0·106	0·082
	16·9	66·2	0·112	
	22·0	33·1	0·073	
	24·5	26·2	0·064	
45	17·3	50·8	0·088	0·062
	21·1	29·4	0·062	
	26·3	23·2	0·061	
	28·7	19·1	0·055	

W = Basis weight, g/m²
r_m = Maximum pore radius, cm

where E is negative and equal to—

$$E = \frac{2\cdot3}{G\sqrt{2}}\,\bar{\tau}w \log\left(1 - \frac{G\bar{\omega}}{w}\left\{1 - \frac{\bar{\tau}w\sqrt{2}}{G\bar{\omega}}\left[1 - \exp\left(-\frac{G\bar{\omega}}{\bar{\tau}w\sqrt{2}}\right)\right]\right\}\right) \; . \;\; (15a)$$

(*see* Appendix).

Table 3 reveals that the differences between the theoretical and calculated values of K have closed somewhat through the use of the modified theory. They may be closed still more by suitably adjusting G, but even now we feel the agreement is good.

TABLE 3—SOFTWOOD SULPHATE II

$^{\circ}$S.R.	W	$r_m \times 10^4$	$r_m W$ (*experimental*)	$r_m W = K$ (*calculated*)	$-E \times 10^4$	$r_m W$ (*corrected*)
16	20·6 34·0 56·0 68·4	62·5 34·6 22·8 18·9	0·129 0·118 0·128 0·129	0·136	1·265	0·133 0·132 0·129 0·127
25	22·3 44·1 80·4 92·1	54·5 23·6 14·3 12·6	0·122 0·104 0·115 0·116	0·130	1·13	0·127 0·125 0·121 0·120
34	17·6 36·7 54·2 73·7	60·6 26·3 18·2 13·4	0·107 0·097 0·098 0·098	0·127	1·11	0·125 0·123 0·121 0·119
44	15·1 31·4 56·6	74·8 27·5 16·4	0·113 0·086 0·096	0·124	1·32	0·122 0·120 0·117

Optical properties

Relative bonded area

AMONG the optical properties of a piece of paper, gloss, brightness, transparency or opacity, the relative amount of optically bonded (or unbonded) area of the external fibre surface area is frequently of first importance. It may be derived in general form from an expression[2] for N_{cm}, the number of fibre crossings in an MP sheet—

$$N_{cm} = N_c' N_L B\left\{\sigma_1 + B\left[1 - \frac{1}{N_L}\right]\left[\sigma_2 + \frac{Cp(0)^2}{1-p(0)^2}\right] - \frac{2Bp(0)^2[1-p(0)^{2(N_L-1)}]}{N_L[1-p(0)^2]^2}\right\}$$

$$(16)$$

where N_c' = number of crossings formed by N_f fibres of no width in one 2-D layer

$B = \frac{1}{2}[1+p(0)]$

$p(0)$ = fractional open area of a 2-D sheet

$= \exp(-N_f\lambda\bar{\omega}/A) = \exp(-G\bar{\omega}/w)$

$\sigma_1(\sigma_2)$ = fraction of possible contacts actually made within (between) contiguous layers = penetration factor

$C = \sigma_K/p(0)^{k-2}$, $K > 2$

σ_k = penetration factor between layers separated by $(K-2)$ other layers.

Equation (16) converts to an expression for the externally bonded area in two steps. Firstly, it must be multiplied by the mean theoretical area per crossing, $\bar{\alpha}_c = (\lambda\bar{\omega})^2/2[\lambda\bar{\omega}+(\lambda+\bar{\omega})^2/\pi] \approx \pi\bar{\omega}^2/2.$ [1] Then it is made to take into account the fraction in optical contact of the total area of the crossings, $(\approx N_{cm}\pi\bar{\omega}^2/2)$, by putting into it factors for the mean fractional bonded area per unit area of crossings between fibres (1) within a layer β_1, (2) between contiguous layers β_2 and (3) in layers separated by $(K-2)$ other layers β_3. These factors are determined, as the σ_k values were earlier, by the technique of Page and Tydeman.[2-4] Assuming $\beta_K/p(0)^{K-2} = \text{constant} = D$, when $K > 2$,[2] introducing $\bar{\alpha}_c$, β_1, β_2 and D appropriately into equation (15) and neglecting terms having N_L in the denominator, because the sheets have many layers, we arrive at an approximate expression for BA, the total amount of optically bonded area on the external surface of the fibres of heavy MP sheets—

$$BA = N_c'N_LB\bar{\alpha}_c\left\{\sigma_1\beta_1+2B\left[\sigma_2\beta_2+\frac{CDp(0)^3}{1-p(0)^3}\right]\right\} \quad . \quad . \quad (17)$$

More useful than an expression for bonded areas is one for the *relative bonded area*, which is equal to BA divided by half the external area of the fibres, $N_LN_f\lambda(\bar{\omega}+\delta) \approx N_LN_f\lambda\bar{\omega}$ for softwood fibres $(\bar{\omega} > \delta)$—

$$RBA = \frac{GB\bar{\omega}}{2w\bar{\tau}^2}\left\{\sigma_1\beta_1+2B\left[\sigma_2\beta_2+\frac{CDp(0)^3}{1-p(0)^3}\right]\right\} \quad . \quad . \quad (17a)$$

In the state of complete interfibre bonding, all values for σ_k and β_k are equal to 1·0 and equation (17a) reduces to an expression for the maximum relative bonded area of an infinitely thick sheet, RBA_{max}, which ought to equal 1·0 at all values of $p(0)$. Calculations have shown RBA_{max} varies somewhat as a function of $p(0)$, being equal to 1·0 only at $p(0) = 0·7$. This non-constancy in RBA_{max} is probably caused by the B term, which is only an approximation to the covering-up effect among the fibres. Such short-

comings in RBA_{max} must also be present, but to a lesser extent, in equation (17a), thereby making it an approximate expression for *RBA*.

A *preliminary* calculation was made of the *RBA* of a bleached sulphite softwood pulp whose *RBA* was also determined by the light scattering technique.* As an arbitrary selection of the basis weight per layer is required, the computation has been repeated three times to demonstrate that the choice has a relatively small effect on the final answer.

Fibre properties

Fibre length	0·258 cm
Fibre width	0·0036 cm
Fibre thickness	0·0005 cm
Curl factor	1·1
Specific fibre weight	$1·9 \times 10^{-6}$ g/cm

Penetration and bonding factors when $G = 1, 2$ g/m²

$\sigma_1 = 1·0; \quad \sigma_2 = 0·9; \quad C = 0·8; \quad \beta_1 = 0·9; \quad \beta_2 = 0·8; \quad D = 0·7$

Penetration and bonding factors when $G = 3$ g/m²

$\sigma_1 = 0·9; \quad \sigma_2 = 0·8; \quad C = 0·8; \quad \beta_1 = 0·9; \quad \beta_2 = 0·8; \quad D = 0·7$

g/m²	p(0)	RBA, %
1	0·83	27 ⎫
2	0·68	35 ⎬ ≈ 30
3	0·57	37 ⎭

The agreement between the theoretical value of 30 per cent and the measured 22 per cent[5] is quite good when account is made for the still approximate nature of our theory and data.

Mechanical properties

Number of fibre-fibre crossing failures
in tensile loading of a 2-D sheet

A MECHANICAL property of paper widely studied in recent years is stress/strain behaviour, for it is important in many applications and more

---

* This pulp was supplied by Dr. W. L. Ingmanson of The Institute of Paper Chemistry, Appleton, Wis., U.S.A., to whom we wish to express our sincere thanks. This pulp was studied because complete physical data including light scattering measurements were available.

subject to theoretical treatment than other properties. It is possible to represent paper as a continuous, homogeneous material and to form theories about it that will embrace given sets of experimental facts. In the past, such theories have seldom shed much light on the phenomena taking place within a sheet under external load and, being based on continuous models, they never have expressed the important *discontinuous* phenomenon of the final rupture of the sheet.

Few paper researchers would deny there are large gaps in our knowledge of the mechanisms of paper behaviour and few would maintain they can be filled without first studying sheet structure. As a first step toward understanding the behaviour of stressed paper as a function of structure, we investigated the rupture of thin 2-D sheets under a tensile load.[6] By straining these sheets with a special device mounted in the holder of a slide projector, we were able to count visually the number of fibre-to-fibre bonds that failed during the rupture. When strained slowly enough, the bonds ruptured individually and each failure was accompanied by a faintly audible signal, a click of sorts. It turned out to be easy to design and carry out an experiment that counted the number of clicks emitted when a 2-D sheet was strained to failure. That apparently identical clicks are associated with the straining of all types of paper, including dense grades like glassine, may mean that the click-counting will acquaint us with the number and rate of bond failures, perhaps fibre failure, when paper is subjected to all types of mechanical loadings (tensile, tear, etc.). Counting clicks may not be very occult, but it could become a fundamental tool for analysing paper failure.

For our first experiments with 2-D sheets prepared from mechanically undamaged fibres as described in detail elsewhere,[1] specimens were mounted in a soundproof chamber with a silent drive to eliminate all motor noise. Straining took place under a microphone whose signals after amplification could be fed variously to a tape recorder (for a permanent record), to a loudspeaker (for demonstration purposes), to an electronic counter and to one pen of a double pen recorder. The output from strain gauges mounted in the stationary clamp holding the specimen was fed to the other pen of the recorder. Not only did both pens record their signals simultaneously, but we were also able to observe visually that each signal—and therefore, each click—corresponded to a bond failure.

Sheets of unbeaten softwood fibres, when strained to complete rupture, show an extremely short (sometimes unobservable) initial period when no crossings fail and a long period when bonds fail, at first sporadically at random over the sheet, then more frequently in what appears as a weaker part of the sheet, finally tailing off until the last bond is broken. We have observed

the failure of ordinary papers to pass through the same phases, but unlike the case of 2-D sheets, bond failure at the main stress relaxation is so rapid that the clicks emitted cannot be recorded by a pen. Nor have we yet learned to distinguish between clicks from crossing failures and those from fibre failures, which are known to occur in ordinary papers. Nevertheless, for any theory of sheet rupture that understands paper as a discontinuous network formed according to statistical laws, the click-counting technique will be an excellent experimental check.

We have developed a theory to predict the number of bonds that must fail to separate a 2-D sheet into two parts. This number of failures is a minimum, because those occurring outside the defined failure zone are not taken into account. Besides this limitation, the theory assumes that all crossings in the failure zone are initially bonded and that no fibres fail.

Consider a 2-D sheet of width l_1 and length l_s divided into n rectangular zones of dimensions $l_1 l_2$. Setting $l_2 < \lambda$, the fibres will on the average be in k zones, that is, split into $\bar{k}$ segments,[1] where—

$$\bar{k} = \frac{2\lambda}{\pi}\left(\frac{1}{l_1}+\frac{1}{l_2}\right)+1$$

In a sheet of N_f fibres, the mean number of fibres per zone is $\bar{n}_f = N_f/n$ and the mean number of fibre segments per zone is—

$$\bar{n}_{\text{seg}} = \bar{n}_f\bar{k}/\bar{\tau}^2$$

The failure zone, which we have assumed to be the only one where crossings fail, is the zone with the fewest segments, $n_{\text{seg min}}$. n_{seg} having a Poisson distribution with mean $\bar{n}_{\text{seg}}$,[1] the expected minimum number of segments in one zone (the failure zone) of a sample of size n is defined by—

$$P(\bar{n}_{\text{seg}}, n_{\text{seg min}}) = \frac{1}{n}^{(4)} \qquad \cdot \quad \cdot \quad \cdot \quad \cdot \quad \cdot \quad (18)$$

where $P(\bar{n}_{\text{seg}}, n_{\text{seg}})$ is the cumulative Poisson distribution. Term $n_{\text{seg min}}$ is the value read from the cumulative Poisson table with the mean $\bar{n}_{\text{seg}}$ and frequency $1/n$.[3]

The mean number of crossings in the failure zone, $\bar{n}_{c\text{ min}}$, is—

$$n_{c\text{ min}} = \tfrac{1}{2} P n_{\text{seg min}} (n_{\text{seg min}} - 1)$$

(*see* Kallmes and Corte, equation (19)[1]) where P, the probability that two segments intersect within the zone, is—

$$P = \frac{\bar{n}_f\bar{\tau}^2(\bar{k}-1)^2}{2l_1 l_2 \bar{k}(\bar{n}_f\bar{k}-\bar{\tau}^2)\left(\dfrac{1}{l_1}+\dfrac{1}{l_2}\right)^2} \qquad \cdot \quad \cdot \quad \cdot \quad \cdot \quad \cdot \quad (19)$$

The only undefined variable of equations (18) and (19), the length of the failure zone l_2, is found from the following considerations. Assuming all bonds have equal strength, the fibres at the failure line will protrude a maximum of half and an average of one fourth of their length. For a random orientation, the projection of the two sections into each other is l_2 or—

$$l_2 = \frac{\lambda}{2\pi} \int_0^\pi |\cos \phi| \, d\phi = \frac{\lambda}{\pi} \qquad . \quad . \quad . \quad . \quad . \quad (20)$$

The number of fibres in the 2-D sheet N_f is calculated from the scanning equation—

$$N_f = \left(\frac{\pi A \bar{\tau}}{2\bar{\lambda}} - l_s\right) \frac{N}{L}$$

where N is the number of fibres intersected in a scan of length L. Before each experiment, three scans were performed 4 mm apart by the technique described.[1]

Results of experiments on 21 samples of 2 g/m² substance are recorded in Table 4. The strips were elongated at 1 mm/min. The independent variables required for computation were $l_s = 1\cdot5$ cm, $l_1 = 1\cdot0$ cm, $\bar{\lambda} = 0\cdot3$ cm, $\bar{\tau} = 1\cdot1$.

TABLE 4

Experiment No.	Experimental results			Calculated values		
	N	N_f	No. of clicks	$\bar{n}_{seg}$	$\bar{n}_{seg\,min}$	$n_{c1\,min}$
1	329	523	216	89	75	205
2	290	461	182	79	66	157
3	316	502	252	86	73	192
4	268	426	216	73	61	133
5	324	515	209	88	74	200
6	340	540	117	92	78	219
7	272	431	119	74	62	138
8	204	323	62	55	44	71
9	254	403	229	69	57	117
10	235	373	165	64	52	99
11	319	506	300	86	73	192
12	328	521	166	89	75	205
13	299	474	258	81	68	166
14	263	418	61	71	59	125
15	289	458	230	78	66	159
16	278	441	221	75	62	140
17	331	526	113	90	76	208
18	298	473	139	81	68	166
19	240	381	159	65	53	102
20	287	456	220	78	66	159
21	316	502	285	86	73	192
Mean			187			160
Standard deviation			67			41

Both being statistical in nature, the theoretical and experimental results of any single sample cannot be compared legitimately, but the agreement between theory and experiment on the average of the 21 results is satisfactory, especially when the minimum nature of the calculated results is taken into account.

Being based on statistical geometry, the click experiment cannot lead to any enumeration of the physical properties of paper. The strength of the individual bonds is an intrinsic property of the material and, as such, has no connection with geometric structure. Once such data and the mechanism of failure are known, the present theory should be a suitable base from which to approximate the strength of networks.

Conclusion

THE geometric structure of paper affects practically all of its physical properties. No theory of geometric structure can, on its own, give a numerical account of the physical behaviour of paper. Some kind of physical information is necessary in every single case. On the other hand, no physical concept or theory, empirical or fundamental, can lead to a real understanding of the behaviour of paper, without taking into account its fibrous structure. Moreover, every geometric approach has to stand the final verification by physical evidence, every physical approach has to be based on the geometric structure in order to be real. The interpretation of physical properties in terms of structure, however, is satisfactorily possible only when the structure itself can be described in a quantitative manner. It has been shown that even a quite incomplete, limited and approximate knowledge of the geometric structure can be used for a quantitative interpretation of physical facts. Every progress in linking together these two aspects should increase our knowledge of, firstly, why paper behaves as it does and, secondly, how to make it behave better.

REFERENCES

1. Kallmes, O. J. and Corte, H., *Tappi*, 1960, **43** (9), 737–752
2. Kallmes, O. J., Corte, H. and Bernier, G., *Tappi*, 1961, **44** (7), 519–528
3. See, for instance, Gumbel, E. J., *Statistics of Extremes* (Columbia University Press, New York, 1958), 75 *et seq.*
4. Scheidegger, A. E., *The Physics of Flow through Porous Media* (Toronto, 1957), 45–46
5. Thode, E. F. and Ingmanson, W. L., *Tappi*, 1959, **42** (1), 74–83; 83–93
6. Corte, H., Kallmes, O. J. and Jarrot, D., *Paper-Maker*, 1961, **142** (7), 61–62, 64–66, 68, 72

Appendix

Derivation of blocking factor

CONSIDER the polygons of one 2-D layer of area A as circular holes whose centres are randomly distributed. The radius r of a circle of area $2g^2/\pi$ [where g is the free fibre length; *see* equations (*17*) and (*18*)[(1)]] is equal to $g\sqrt{2}/\pi$. A fibre of dimensions $\lambda\omega$ dropped randomly on to A blocks a hole of radius r completely when the fibre centre lies within a rectangle of area $(\lambda - 2r)(\omega - 2r) \approx \lambda(\omega - 2r)$ and $2r \leq \omega$.

prob. (hole blocked) = prob. [fibre centre in rectangle $\lambda(\omega - 2r)$]
$\times$ prob. $(2r \leq \omega)$.

prob. (fibre centre in rectangle) $= \dfrac{\lambda}{A}(\omega - 2r)$.

prob. $(2r \leq \omega) = \kappa \displaystyle\int_{2r=0}^{2r=\omega} e^{-2\kappa r}\, d(2r)$

where

$$\kappa = \frac{1}{2r} = \frac{\pi}{2\sqrt{2}\bar{g}} = \frac{\pi}{2\sqrt{2}}\left(\frac{N}{L}\right) \qquad . \quad . \quad . \quad . \quad (I\text{-}1)$$

Hence—

prob. (hole blocked) $= \dfrac{\lambda\kappa}{A} \displaystyle\int_{2r=0}^{2r=\omega} (\omega - 2r)e^{-2\kappa r}\, d(2r)$

The number of holes in the first layer covered by N_f fibres of the second layer n_{c_1} is—

$$n_{c_1} = \frac{N_f n\lambda\kappa}{A} \int_{2r=0}^{2r=\omega} (\omega - 2r)e^{-2\kappa r}\, d(2r)$$

$$= \frac{N_f n\lambda}{A} \left[\omega - \frac{1}{\kappa}(1 - e^{-\kappa\omega})\right]$$

$$= qn$$

The number of open passages through two layers is—

$$n_2 = n(1 - q)$$

through three layers—

$$n_3 = n(1 - q)^2$$

and through m layers—

$$n_m = n(1-q)^{m-1}$$
$$\approx n(1-q)^m = N_h(1-q)^m$$

The term n_m replaces N_h in equation (12) yielding—

$$r_m W = \frac{1}{\sqrt{2}} \bar{\tau}w \log_e [N_h(1-q)^m]$$

$$= K + EW \qquad . \quad . \quad . \quad . \quad . \quad . \quad . \quad . \quad . \quad (15)$$

where K is from equation (12) and—

$$E = \frac{1}{\sqrt{2}} \frac{\bar{\tau}w}{G} \log_e (1-q)$$

$$= \frac{2 \cdot 3}{G\sqrt{2}} \bar{\tau}w \log \left(1 - \frac{G\bar{\omega}}{w} \left\{1 - \frac{\bar{\tau}w\sqrt{2}}{G\bar{\omega}} \left[1 - \exp\left(-\frac{G\bar{\omega}}{\bar{\tau}w\sqrt{2}}\right)\right]\right\}\right). \quad (15a)$$

Note that—

$$m = \frac{W}{G}, \quad \kappa = \frac{\pi}{2\sqrt{}} \left(\frac{N}{L}\right) \text{ and } \frac{N}{L} = \frac{2\bar{\lambda}N_f}{\pi A} = \frac{2G}{\pi w}.$$

DISCUSSION

MR. D. H. PAGE: In the multi-planar theory presented in your earlier paper, you have considered the distribution of bonding that arises when two 2-D sheets are separated by a third (Fig. D9). I believe I am right in saying that you have defined a factor for the probability that crossings between the lower and upper layer are bonded and that you have used this factor to obtain the distribution of distances between bonded crossings in a multi-planar sheet. There are sound physical reasons that this treatment is unsatisfactory. By defining a probability factor that is constant over the whole sheet, it is implied

_____ Fibres of middle layer
_._._.- Fibres of upper layer
_ _ _-- Fibres of lower layer
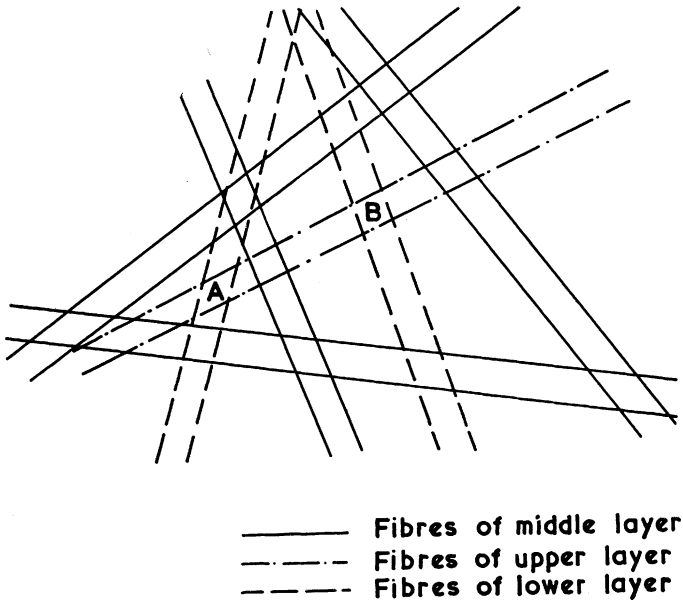
Fig. D9

that the two fibres of the first and third layer crossing over a small opening of the second layer have the same chance of bonding to one another as have two fibres crossing over a large opening. This is not a physically justifiable assumption. The factor controlling whether or not bonding occurs between the first and third layer is not only the flexibility or plasticity of the fibres, but also the length of the span over which the fibres are free to deflect.

Thus, it is clear that crossing *B* (Fig. D9) has a much greater chance of being bonded than crossing *A*. This effect will control to a large extent the shape of the distribution of distances between centres of bonded crossings.

While the negative exponential curve for gap length is correct for the distances between *all* crossings, it will be radically modified when the distances between *bonded* crossings are considered. The effect will be to decrease the number of short distances between bonded crossings, also to decrease the number of very large distances. Our own experimental values, obtained on one side of the fibre only in a sheet (the side facing inwards towards the body of the sheet), show this effect clearly. Fig. D10 gives the experimental values of
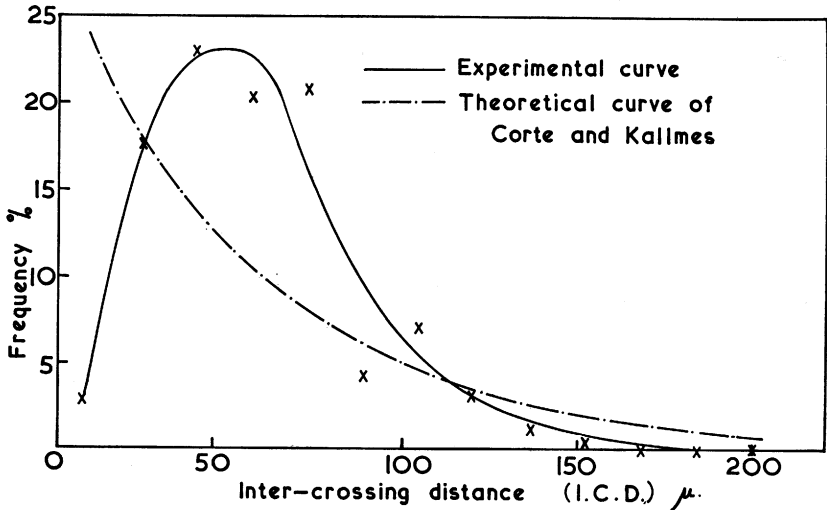
Fig. D10

intercrossing distance, together with the theoretical negative exponential curve fitted to give the same mean I.C.D. Whereas the negative exponential predicts that about 8 per cent of the distances will be greater than 150—in fact, none are observed in 188 readings. This sharp cut-off of high intercrossing distances is of importance in considering the theory of Kallmes for the elasticity of paper, since it is necessary for his theory that high intercrossing distances with their high potential extension in bending should exist.

While I realise that your model of paper had to be simplified to permit a mathematical treatment, I think it is a dangerous position when the mathematics enforce assumptions that are not physically justifiable and particularly so when attention is not drawn to them.

Secondly, I would like to ask how many clicks you hear, when a sheet of normal basis weight is extended to failure, compared with the number of fibre-to-fibre bonds in the sheet. We find that, in the surface, of the order of 5 per cent of fibre-to-fibre bonds separate completely. It would be interesting to have evidence of total fibre separation within the body of the sheet. In such a tightly bonded state, we believe there is the possibility that total bond breakage is very infrequent.

DR. O. J. KALLMES: The term B is not a probability factor: it is the experimentally determined fraction of the crossings bonded and, as such, has to give the correct mean free fibre length. The distribution of (g_m) *inside* the sheet can only be assumed at present.

Your description of our experiment is correct. I consider your experiment measuring the free fibre length *on the surface* is at least as suspect as our mathematical approximations. It is presumably impossible to measure the mean free fibre length in a sheet; the only test possible is to use the calculated value and apply it in a physical experiment. We have done this in our second contribution in two entirely different experiments, a porous and an optical. The good checks obtained between theory and experiment lend considerable support to the mean free fibre length of the entire sheet.

DR. H. CORTE: All we do is to measure the fraction of those bonds that see each other and are bonded. We do not call this fraction probability (because it has nothing to do with mathematics), but the bonded fraction of those bonds that see each other (symbol σ) and the free fibre length does not come into play at all. It turned out that the factor σ is roughly proportional to the open area. We have no idea why this is so—in fact, we know that it is not so, but it is good enough as an approximation. No mathematical assumptions have been made here, only experiments. The values are independent variables that have to be measured and cannot be computed. Once they have been determined, however, we are not satisfied by merely tabulating or plotting them. Instead, we use them for further quantitative evaluation of sheet properties.

The number of clicks depends, of course, on the size of the sample and on the basis weight—that is, the number of fibres present (you said 10^7). The number of clicks you hear depends not only on the number of bonds present, but on the shape of the sample. The film shown allowed the actual counting of the clicks, because they could be recorded on a tape recorder and played back. For thicker sheets, the clicks are too numerous and too fast to be recorded reliably on any mechanical instrument, but we have fed the output

into an electronic counter that counts up to 2 000 pulses per second and there is a programme on at the moment. I am not quite sure, but in the last experiment I saw myself (with a sheet of about 25 g/m², say, 8 mm wide and 10 mm long) the number of clicks was about 1 500. We will refer to that in due course. In a 2-D sheet, the total number of bonds in a sample of that kind was about 4 000 and the number of clicks averaged about 180—that is, the number of broken bonds averaged 180—and the application of extreme value theory gives at best only the number of bonds that break along the breaking zone. In other words, the value should always be lower than the observed value, because no theory so far produced permits calculation of the extra bonds that break at random all over the sample.

PROF. A. H. NISSAN: I think Corte is absolutely correct that a fracture is discontinuous in paper. Where I take issue with him is his suggestion that a fracture is continuous anywhere else. It is a matter of time scale, also of energy amplifications. At the moment, we are studying at Rensselaer the actual straining of minute crystals under the electron microscope at very high resolution by observing the motion of dislocations. This, to all outward appearances, would give a clear case of continuity as your click on the cellulose film indicated, because it is crystal. It is not so. If you amplify enough to get the machine and apparatus commensurate with the phenomena being measured, it is found to be discontinuous. There is danger in assuming that we can use only one system of experimentation in the study of phenomena of a wide range. The flow of air at atmospheric pressure appears perfectly continous and the theory of viscous flow applies. The flow of air at 10^{-6} atm in wide tubes is discontinuous. You can 'count' the units. Now, supposing the enthusiastic physicist shows that the flow of air at 10^{-6} atm is discontinuous: he is perfectly correct, but I maintain that to study only that is to miss the opportunity of discovering viscous flow. This is very important, because flow at atmospheric pressure is continuous by ordinary scale. I suggest that the click heard when a fibre bond is breaking is comparable to the click heard when cellulose film breaks. Here, you have extended it commensurate with fibre length and fibre area, but with cellulose film you are not dealing with the same scale. There is some danger if we get too enthusiastic for one method: we might miss another aspect of truth by saying, 'Only this will work'.

DR. CORTE (*written contribution*): In my report yesterday of our first contribution, I stressed the importance of the structural scale. The scale reaches from the foil-like apparent continuity of larger samples of paper under certain experimental conditions to the molecular discontinuity of hydrogen bonds.

Each level is equally important. When we consider the structure to consist of undistinguishable fibres as elements, we do so because this viewing angle has been neglected. We think that such a treatment yields a new and useful insight into a number of interesting and important paper properties. We do not claim, however, that our method, though very powerful, is the only one to tell the whole truth.

MR. P. G. SUSSMAN: Referring to Fig. 3 and Fig. 4, Kallmes has confirmed that the ends of the curves show the actual breaking loads of the MP sheets and the normal handsheets? This being so, the tensile behaviour of the MP and 'normal' sheets is surprisingly similar.

I, too, have made sheets from a fibre suspension of very low consistency, 0·002 per cent, but 60 g/m² in substance, draining all the water through the sheetmachine in one go; one sheet took about 5 min to make. The 'random structure' sheets that I made had a slightly lower burst factor than had corresponding normal handsheets formed from 0·02 per cent stock. I had expected to make a better sheet than a normal handsheet.

In my 'random sheet' experiments, the amount of fibres lost through the wire was measured and found to be about 5 per cent of the total sheet weight, similar to the losses occurring with normal handsheets. If any fractionating took place in Kallmes' sheetmaking, I do not know what effect that would have.

DR. KALLMES: My only comment is that we made a large number of tests and the results were generally quite close. For heavier sheets, the differences became smaller, essentially alike within 10 per cent; on the two-layer sheets, there were some appreciable differences (indicated in the figures, especially Fig. 3).

In all our work to date, we have screened the pulp beforehand to deal only with the long fibre fraction: thus, no fines effect was added.

DR. J. KUBÁT: I have three comments on points discussed during the lectures today.

1. Bond breaking during straining—The concept of bond breaking must always be seen against the background of the relation between the number of bonds in the sheet and its modulus of elasticity. Irrespective of the actual form of this relationship, it can easily be demonstrated that the modulus is nearly constant along the whole stress/strain curve. Furthermore, when variations occur, there is always an increase in the modulus. The main part of the stress/strain curve is due to plastic flow, which takes place only during loading.

When deloading, the deformation is a superposition of an elastic and visco-elastic component. The slope of the stress/strain curve after the reversal of the straining procedure is thus identical with the modulus at the actual rate of straining. Another method of studying the magnitude of the modulus along the stress/strain curve is a combination of a constant rate of straining with a sinusoidal deformation of suitable frequency and amplitude. Experiments of this kind have been done at the Swedish Forest Products Research Laboratory in Stockholm. Different types of paper were investigated for modulus changes following straining, but no decrease could ever be observed.

2. *Inner stresses in the sheet*—Theories treating the sheet as a statistical assembly of interconnected fibres cannot (mainly for mathematical reasons) include the inner stresses, which are usually present in all types of paper. The magnitude of these stresses is by no means a matter of academic interest only. We could in fact demonstrate, mainly by measuring stress relaxation at different stress levels, that the inner stresses can reach values of 30–50 per cent of the tensile strength.

3. *Fluctuations, particularly of the stress during deformation* (*audible clicks, observed by Corte*)—The audible clicks heard during the straining of a strip of paper represent one of several different effects following from the discontinuity of the straining process on the microscopical scale. Apart from the fact pointed out by the Chairman that Corte's experiment much more reflected the conditions of a rupture process in tear in the sheet, there is no doubt that observations of the discontinuous nature of the deformation of the sheet represent a powerful means of getting direct insight into the kinetics of paper rheology. There are, of course, several methods of doing that. At our laboratory, we have chosen the measurement of electrical fluctuations. Such fluctuations can be measured with or without a direct current flowing through the strip. In the latter case, we found intense noise phenomena within the plastic region of the stress/strain process. The noise was not present in the elastic region and, furthermore, it disappeared when the contraction of the strip from the state of plastic flow began. We consider this another demonstration of the existence of at least two different flow mechanisms in paper—delayed elastic (visco-elastic) and plastic flow. There are still more methods for following the discontinuities in straining solid materials. One of them is the direct measurement of the microscopical stress increments by sensitive piezoelectric devices. In that way, it has been possible to show that, in the straining of metal crystals, the number of clicks is identical with the number of strain lines formed during the actual deformation, revealed and counted under electron microscope magnification.

All these examples demonstrate clearly that problems in connection with the deformation and flow of paper are amenable to direct observation on the microscopical scale. The coarse structure of a paper sheet, compared with the structure of a metal, makes such measurements still easier to carry out.

DR. KALLMES: My one comment is that the mechanical model used in this elasticity equation is very simple. The object of the exercise was to see if the structure theory could be applied at all—that is, if you can relate the properties of fibres and paper through arrangement of the fibres in the sheets. The mechanical model used is extremely simple, though we realise it has shortcomings.